

# Maximum Likelihood based Direct Position Estimation for Mobile Stations in Dense Multipath

Alessio Fascista, Angelo Coluccia, *Senior Member, IEEE*, and Giuseppe Ricci, *Senior Member, IEEE*

## Abstract

The problem of direct position estimation in dense-multipath mobile scenarios is addressed. A low-complexity, fully-adaptive algorithm is proposed, based on the maximum likelihood approach. The processing is done exclusively on-board at the mobile node by exploiting the training sequence of a narrowband radio signal; thus, an antenna array is required only on the mobile node, as opposed to MIMO approaches where multiple antennas are considered at both sides. The proposed algorithm is able to estimate via adaptive beamforming (with spatial smoothing for coherence decorrelation) the optimal projection matrix that makes the received signal orthogonal to the multipath subspace; in addition, it tracks line-of-sight associations over the trajectory, hence achieving an integration gain. A simpler variant of the algorithm is also devised, which does not require any training sequence, at the price of some accuracy loss. The performance assessment shows that the proposed algorithms are very effective in (dense) multipath conditions, significantly outperforming natural competitors also when the number of antennas and snapshots is kept at the theoretical minimum.

## Index Terms

Direct position estimation (DPE), angle of arrival (AOA), maximum likelihood (ML), mobile localization

## I. INTRODUCTION

Position estimation is important in many contexts such as wireless sensor networks, vehicular scenarios, and for navigation/tracking at large. Locating a node in a wireless system involves radio signals propagating between the node and a number of base stations (BSs) in known positions. Different information can be exploited, namely received signal strength (RSS), time (difference) of arrival (TOA/TDOA), and angle of arrival (AOA) [1]–[4]. Techniques based on the RSS, although typically simpler, are not able to provide sufficient location accuracy due to the great variability of the power in wireless channels, especially in case of strong multipath. On the other hand, time of arrival (TOA) [5] or time difference of arrival (TDOA) [6], [7] techniques are challenging in terms of clock synchronization and are very sensitive to multipath. AOA-based localization has gained more attention in recent

All authors are with the Dipartimento di Ingegneria dell'Innovazione, Università del Salento, Via Monteroni, 73100 Lecce, Italy. E-Mail: name.surname@unisalento.it

years due to the widespread of MIMO technologies in 4G/LTE cellular networks, and is even more attractive for future 5G mmWave scenarios in which array size significantly shrinks hence can be integrated in mobile terminals (smartphones) [8]. Interestingly, the multipath environment for mmWave is sparse in angle [9], which reduces the complexity of the localization task in this respect; on the contrary, localization based on more conventional radiofrequency signals (cmWave) is made challenging by the presence of dense multipath effects that dramatically affect all types of information (RSS, TOA, AOA), although in different ways.

Localization approaches can be either direct or indirect. Indirect positioning are suboptimal techniques which first obtain some position-related information, namely distances or angles, and then combine them to estimate the unknown position [10]. Although popular due to their reduced complexity (e.g., for low-cost WSNs [11]), their accuracy is usually limited, and also some bias may be introduced by the first estimation step [12]. Direct position estimation (DPE) techniques, as opposed to such two-step location methods, use a single-step approach to estimate the location directly from the raw signals. In so doing, the constraints between the collected measurements and the node positions are explicitly included in the position estimation, resulting in a significant improvement of the achievable performance [13], [14].

In static scenarios, maximum likelihood (ML) DPE has been developed for a single-path channel in which the multipath effect is modeled as additive noise [15], [16], then extended to multiple nodes localization [17]. The minimum-variance distortionless response-based DPE method proposed in [18], [19] has better resolution and immunity to jamming and interference, but its performance tends to degrade at low SNRs. DPE methods tailored to special signals such as orthogonal frequency division multiplexing (OFDM), cyclostationary signals, and intermittent emissions have also been proposed [20]–[22]. In [23] a ML direct location estimator using wideband signals for nodes in the near field of the sensor array is derived. In [24], a TOA-based DPE technique is proposed for operating in dense multipath environments, but it requires knowledge of the power delay profile, and is limited to localization of a static node. A novel TOA-based direct localization technique for multiple nodes based on ideas of compressive sensing and atomic norm minimization has been recently proposed in [25].

As mentioned, with the widespread of MIMO technologies, AOA-based DPE algorithms are gaining momentum; in particular, massive arrays offer the possibility of precisely estimating the parameters of each individual multipath component thanks to their high angular resolution. A ML estimator has been developed in [26] for localizing a single node assuming a fixed and known number of multipaths, but without providing an efficient way to compute the estimator. Recently, a novel algorithm called direct source localization (DiSouL) has been proposed [27]: it is based on a compressed sensing framework that exploits some channel properties to distinguish LOS from NLOS signal paths, leading to superior performance compared to other approaches. However, at more conventional radiofrequencies (cmWave), the multipath is not always resolvable; moreover, standard AOA estimation approaches are inapplicable because of the coherence among the received multiple paths that originate from the same signal.

It is also worth noticing that DPE algorithms typically assume spatially-dispersed arrays, i.e., in macro diversity. They process the collected data at a central node to which all the sampling data are transferred, considerably increasing the bandwidth consumption [28]. To this aim, a dedicated infrastructure is necessary for their effective implementation, thus limiting their applicability to a restricted range of scenarios. Furthermore, all the DPE

algorithms cited above focus on the one-shot estimation problem, i.e., they do not consider kinematic aspects related to node mobility but rather solve the localization problem at any fixed instant as in a static case.

In this paper, we present a novel DPE algorithm for dense multipath scenarios under mobility. In particular, the proposed approach has low complexity and is fully adaptive, i.e., it does not require any tuning or additional information about the environment. To the best of our knowledge, this is the first general AOA-based DPE algorithm that can cope with dense multipath and exploit mobility at the same time. The processing is done exclusively on-board at the mobile node by using the training sequence of a narrowband radio signals, without any increase in the bandwidth consumption, and requiring an antenna array only on the mobile node (as opposed to MIMO approaches where multiple antennas are considered at both sides). The proposed approach does not require the deployment of a new infrastructure, and is effective also with a single BS; furthermore, it outperforms natural competitors also when using a minimal number of antennas and snapshots. The main idea is to estimate via adaptive beamforming the optimal projection matrix that makes the received line-of-sight (LOS) signal orthogonal to the multipath subspace, thus obtaining a good approximation of the likelihood function; in addition, tracking of LOS associations over the trajectory is performed, yielding an integration gain. A simpler variant of the algorithm is also devised, which does not require any training sequence, at the price of some accuracy loss.

The rest of the paper is organized as follows. In Sec. II we introduce the system model and describe the reference scenario. In Sec. III we formulate the estimation problem and illustrate in details the design and derivation of the proposed DPE algorithms. Then, in Sec. IV, we analyze the performance, also in comparison with natural competitors, by means of Monte Carlo simulations in different realistic scenarios. We conclude the paper in Sec. V.

## II. SYSTEM MODEL

We consider, as a reference scenario,  $N_{BS}$  BSs located in fixed, known positions and a mobile station (MS) with unknown position. The MS moves along an arbitrary trajectory, with (generally non-constant) velocity that is measured through an inertial sensor or odometer, as typically available in a vehicle or in a smartphone. Thus, we will assume at the design stage that velocities are known, but their estimates will be used in the implementation of the algorithms.

The 2D position of the  $b$ -th BS and of the MS at a given time instant  $t$  are denoted by  $\mathbf{p}_{BS}^b = [x_{BS}^b \ y_{BS}^b]^T$  and  $\mathbf{p}(t) = [x(t) \ y(t)]^T$  (where  $^T$  is the transpose operator), respectively, where  $b \in \mathcal{B}$  and  $\mathcal{B} = \{1, 2, \dots, N_{BS}\}$  is the set of univocal identifiers of the BSs. In the considered case, and differently from many other localization setups, the BSs are transmit-only (with a single, typically omnidirectional antenna) while the MS is receive-only and equipped with an  $M$ -element uniform linear antenna array (ULA). Particularly, each BS periodically broadcasts a signal with baseband representation  $s(t) = \sum_h c_h g(t - hT)$  where  $g(\cdot)$  denotes a root-raised-cosine (RRCR) signaling pulse known to the receiver,  $c_h s$  are the transmitted symbols, and  $B = (1 + \alpha_{\text{RRCR}})/2T$  is the one-sided bandwidth with roll-off factor  $\alpha_{\text{RRCR}} \in [0, 1]$ . Notice that the derivations would apply also to the reverse situation in which the MS is transmitting and the BSs are receiving; this is however less attractive since it requires additional mechanisms to coordinate data collection, including BS synchronization.

The MS executing the proposed localization algorithms collects and processes the impinging signals coming from the transmitting BSs nearby, the latter assumed to be in the far field with respect to the MS. More specifically, let  $\mathbf{p}_0 = [x_0 \ y_0]^T \stackrel{\text{def}}{=} \mathbf{p}(t_0)$  be the (unknown) MS position at time instant  $t_0$  when the localization procedure starts. Moreover, let  $t_i, i > 0$ , denote the time instant at which a signal transmitted by one of the BS has been received; we denote by  $b_i \in \mathcal{B}$  the identifier of such a BS. Since there is a correspondence between the  $i$ -th received signal and the transmitting BS  $b_i$ , in the following we will use only  $t_i$  while omitting  $b_i$  from the notation. As concerns the multipath channel, we assume that (i)  $T$  is much greater than the channel delay spread  $\tau_S$ , so that the channel exhibits a constant complex gain response; (ii)  $B$  is much greater than the channel Doppler spread  $B_D$  caused by MS mobility, so that the channel response can be assumed to be time-invariant over a small-scale observation period  $T_{obs}$ . The resulting received signal over a generic time interval  $[t_i, t_i + T_{obs}]$  after down-conversion, clock and frequency/phase offsets recovery can be expressed as [29], [30]

$$\mathbf{x}(t) = \gamma_i(\mathbf{x}_i^{\text{LOS}} + \mathbf{x}_i^{\text{NLOS}})s(t) + \mathbf{n}(t) \quad t_i \leq t \leq t_i + T_{obs} \quad (1)$$

where

$$\mathbf{x}_i^{\text{LOS}} = \mathbf{a}(\theta_i^{\text{LOS}}) \quad (2)$$

$$\mathbf{x}_i^{\text{NLOS}} = \sum_{m=1}^{D_i} \beta_i^m \mathbf{a}(\theta_i^m) \quad (3)$$

in which  $\mathbf{n}(t)$  is thermal noise and  $\mathbf{a}(\theta)$  is the steering vector representing the array response for a signal impinging with angle  $\theta$ . As to  $\gamma_i$  and  $\theta_i^{\text{LOS}}$ , they are the complex amplitude coefficient related to large-scale fading (or path-loss) and the AOA of the LOS path at time instant  $t_i$ , respectively, while  $\beta_i^m$  and  $\theta_i^m$  are the complex small-scale fading coefficient and the AOA of the  $m$ -th multipath component out of the  $D_i$  non-line-of-sight (NLOS) paths. Notice that the value of  $D_i$  is arbitrary for each time instant  $t_i$ ; in the following we assume that its value can be set (even in a conservative way) based on preliminary considerations.

It is worth highlighting that this model describes a multipath channel with *flat* and *slow* fading effects. Notice that (i)  $T \gg \tau_S$  is tantamount to neglecting the delays  $\tau_i^m$ s associated to the  $D_i$  NLOS paths, that is,  $s(t - \tau_i^m) \approx s(t) \forall m$ , while (ii)  $B \gg B_D$  guarantees that the complex coefficients  $\beta_i^m$ s do not change over the observation period  $T_{obs}$ . It is also assumed that  $T_{obs}$  is short enough so that the position and velocity of the MS remain approximately constants, i.e., the multipath geometry in terms of  $\theta_i^{\text{LOS}}$  and  $\theta_i^m$ s is unchanged. The way the parameters  $B$  and  $T_{obs}$  are chosen will be discussed in the numerical analysis conducted in Sec. IV (and Appendix), where a realistic scenario of MS localization in multipath environments is considered.

For  $\mathbf{n}(t)$  we consider the classical white complex normal model with covariance matrix  $\mathbf{R}_n = \mathbb{E}[\mathbf{n}(h)\mathbf{n}^H(k)] = \sigma^2 \mathbf{I}_M \delta_{hk}$  (where  $^H$  is the Hermitian operator),  $\sigma^2$  denoting the noise power,  $\mathbf{I}_M$  the  $M \times M$  identity matrix, and  $\delta_{hk}$  the Kronecker symbol. Moreover, for a ULA with isotropic antennas (and no mutual coupling), as the one we are assuming here, the steering vector  $\mathbf{a}(\theta)$  can be expressed as

$$\mathbf{a}(\theta) = \left[ 1 \ e^{j\omega d \sin \theta} \dots e^{j(M-1)\omega d \sin \theta} \right]^T \quad (4)$$

where  $\omega = 2\pi/\lambda$  represents the incident wave number,  $\lambda = c/f_c$  is the carrier wavelength,  $f_c$  is the carrier frequency,  $c$  is the speed of light, and  $d = \lambda/2$  is the ULA interelement spacing. Throughout the rest of the paper, we assume that all the parameters  $\gamma_i$ ,  $\theta_i^{\text{LOS}}$ ,  $\beta_i^m$ s,  $\theta_i^m$ s are unknown.

At the receiver,  $\mathbf{x}(t)$  is passed through a matched filter

$$\mathbf{y}(t) = \int_{t_i}^{t_i+T_{\text{obs}}} g^*(\tau-t)\mathbf{x}(\tau)d\tau \quad (5)$$

(where  $*$  is the complex conjugate operator), whose output is then sampled at a rate  $f_s = 1/T$ , resulting in the following sequence of received samples

$$\mathbf{y}_{i,n} = \gamma_i(\mathbf{x}_i^{\text{LOS}} + \mathbf{x}_i^{\text{NLOS}})c_{i,n} + \boldsymbol{\nu}_{i,n} \quad n = 0, \dots, N-1 \quad (6)$$

with  $N = \lfloor \frac{T_{\text{obs}}}{T} \rfloor$  the number of samples,  $c_{i,n}$  the discrete symbol related to the  $n$ -th sample taken at  $t_{i,n} = t_i + nT$ , and  $\boldsymbol{\nu}_{i,n} \sim \mathcal{CN}_M(\mathbf{0}, \sigma^2 \mathbf{I}_M)$  the filtered thermal noise<sup>1</sup>. We assume that the symbols are known to the receiver, which is usually obtained by considering the first part of the transmission where a known training sequence is inserted for channel estimation and synchronization purposes [31]<sup>2</sup>. Hereafter, we denote with  $\mathbf{Y}_i = [\mathbf{y}_{i,0} \cdots \mathbf{y}_{i,N-1}]$  the  $M \times N$  matrix containing samples of the  $i$ -th observation. It is worth noting that the AOA of the LOS path  $\theta_i^{\text{LOS}}$  directly relates the position of BS  $b_i$  to the MS position through

$$\theta_i^{\text{LOS}} = \text{atan2}\left(y_B^{b_i} - y(t_i), x_B^{b_i} - x(t_i)\right) \quad (7)$$

where the function  $\text{atan2}(y, x)$  is the four-quadrant inverse tangent, and the angle is measured counterclockwise with respect to the  $x$ -axis, as depicted in Fig. 1.

For a sufficiently high BSs send rate (e.g.,  $R_{BS} \geq 10$  Hz), it is reasonable to assume that the time interval between any two consecutive observations is relatively short ( $\leq 100$  ms). As a consequence, the (arbitrary) MS trajectory over  $[t_0, t_k]$ ,  $k \geq 1$  can be approximated by the following kinematic model

$$\mathbf{p}(t_k) = \begin{bmatrix} x(t_k) = x_0 + \sum_{i=1}^k v_x(t_{i-1})(t_i - t_{i-1}) \\ y(t_k) = y_0 + \sum_{i=1}^k v_y(t_{i-1})(t_i - t_{i-1}) \end{bmatrix} \quad (8)$$

where a constant velocity vector  $\mathbf{v}(t_i) = [v_x(t_i) \ v_y(t_i)]^T$  is considered for  $t \in [t_i, t_{i+1})$ , read from the onboard sensors at time instant  $t_i$ . For the sake of exposition, we consider without loss of generality a Cartesian reference system in which the motion is always parallel to the  $y$  axis. It is worth noting that a generic trajectory can be realigned to such an equivalent reference system by performing, at each time instant  $t_i$ , a rotation of the MS local reference system equal to the heading vector, the latter obtained from the measured velocity  $\mathbf{v}(t_i)$ .

Differently from most state-of-art approaches which are based on one-shot solutions, our approach adds one more dimension to the localization procedure, namely the variation in time. Thus, although more unknown parameters may need to be estimated, each collected  $\mathbf{Y}_i$  brings a new position-related information that can help the MS to reconstruct its most probable trajectory over time. Following this idea, two direct position estimation (DPE) algorithms to localize a MS in presence of multipath are derived.

<sup>1</sup>Without loss of generality, we consider a signaling pulse with normalized energy, i.e.,  $\int_{t_i}^{t_i+T_{\text{obs}}} |g(\tau)|^2 d\tau = 1$ .

<sup>2</sup>A decision-directed approach should also be possible, but is beyond the scope of the present contribution.

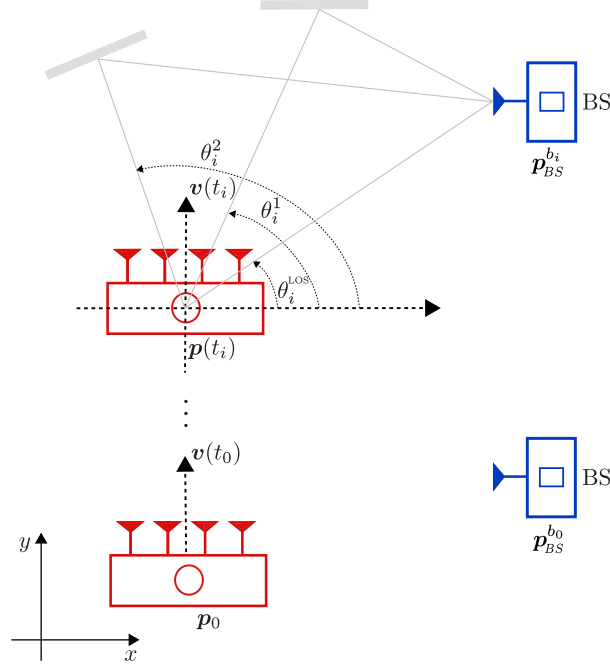


Fig. 1: Reference scenario of the considered mobile position estimation problem.

### III. DIRECT POSITION ESTIMATION

In this section, we propose novel DPE algorithms for the system model presented in Sec. II. Let  $\mathcal{Y} = \{\mathbf{Y}_1, \dots, \mathbf{Y}_K\}$  denote the set of observations available up to the current time instant  $t_K$ . Assuming that the velocities of the MS are known — estimates from the onboard sensors will be used in practice, so we will include velocity errors in the simulations of Section IV — the localization problem reduces to the estimation of the MS (initial) position  $\mathbf{p}_0$ , but embedded in a problem with many nuisance parameters due to multipath propagation.

#### A. ML-based Direct Position Estimation

We observe that each sample vector  $\mathbf{y}_{i,n}$ ,  $1 \leq i \leq K$ ,  $0 \leq n \leq N-1$ , is statistically characterized as

$$\mathbf{y}_{i,n} \sim \mathcal{CN}_M(\gamma_i(\mathbf{x}_i^{\text{LOS}} + \mathbf{x}_i^{\text{NLOS}})c_{i,n}, \sigma^2 \mathbf{I}_M) \quad (9)$$

where all parameters are treated as deterministic unknowns, except the symbols  $c_{i,n}$ s, which we recall are assumed known at the receiver. More precisely, the whole set of unknowns includes  $\mathbf{p}_0$ , which represents the parameter of interest, and  $\boldsymbol{\psi} = (\sigma^2, \boldsymbol{\gamma}, \boldsymbol{\xi})$  which denotes the vector of nuisance parameters, with  $\boldsymbol{\gamma} = [\gamma_1 \dots \gamma_K]^T$ , and  $\boldsymbol{\xi} = [\boldsymbol{\beta}^T \ \boldsymbol{\theta}^T]^T$ , with  $\boldsymbol{\beta}^T = [\beta_1^1 \dots \beta_1^{D_1} \dots \beta_K^1 \dots \beta_K^{D_K}]$ , and  $\boldsymbol{\theta}^T = [\theta_1^1 \dots \theta_1^{D_1} \dots \theta_K^1 \dots \theta_K^{D_K}]^T$ . The ML direct position estimator is then given by

$$\hat{\mathbf{p}}_0 = \arg \max_{\mathbf{p}_0} \left[ \max_{\boldsymbol{\psi}} L(\tilde{\mathbf{p}}_0, \tilde{\boldsymbol{\psi}}) \right] \quad (10)$$

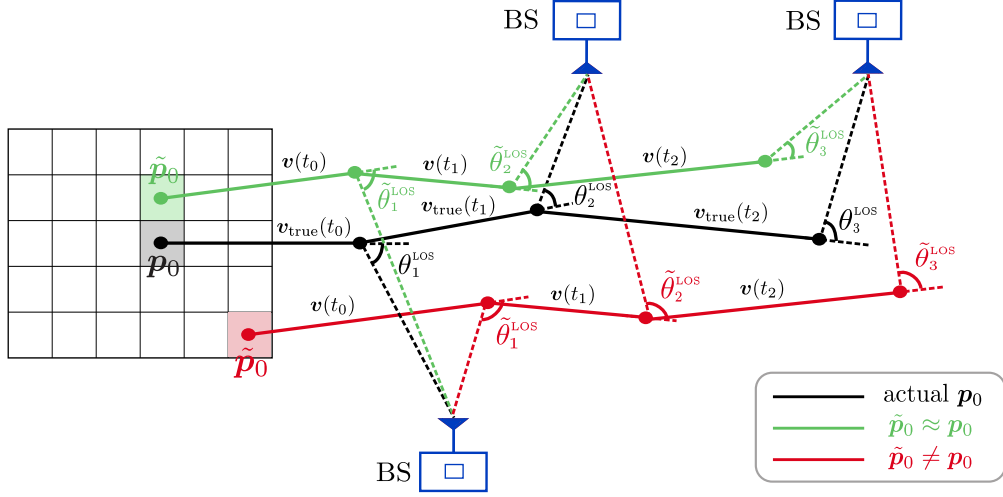


Fig. 2: Example of trajectory/angle reconstruction up to  $K = 3$  for two different values of the trial position  $\tilde{\mathbf{p}}_0$  in comparison with the true trajectory for  $N_{BS} = 3$ .

where  $L(\tilde{\mathbf{p}}_0, \tilde{\boldsymbol{\psi}}) \stackrel{\text{def}}{=} \log(f(\mathcal{Y}|\tilde{\mathbf{p}}_0, \tilde{\boldsymbol{\psi}}))$  and  $f(\cdot)$  denotes the probability density function of the observations  $\mathcal{Y}$  given  $\tilde{\boldsymbol{\psi}}$  and an initial position  $\tilde{\mathbf{p}}_0 = [\tilde{x}_0 \ \tilde{y}_0]^T$ . From (9) it follows that

$$L(\tilde{\mathbf{p}}_0, \tilde{\boldsymbol{\psi}}) = - \left[ MKN \log(\pi \tilde{\sigma}^2) + \frac{1}{\tilde{\sigma}^2} \sum_{i=1}^K \sum_{n=0}^{N-1} \|\mathbf{y}_{i,n} - \tilde{\gamma}_i(\tilde{\mathbf{x}}_i^{\text{LOS}} + \tilde{\mathbf{x}}_i^{\text{NLOS}})c_{i,n}\|^2 \right] \quad (11)$$

where  $\|\cdot\|$  denotes the vector norm. It is worth noting that for a given position trial  $\tilde{\mathbf{p}}_0$ , the AOAs of the LOS paths  $\{\tilde{\theta}_i^{\text{LOS}}\}_{i=1}^K$  are readily determined from the computation of  $\{\tilde{\mathbf{p}}(t_i)\}_{i=1}^K$  through (8), followed by the application of the geometric model in (7). On the other hand, relating the nuisance parameters  $\tilde{\boldsymbol{\psi}}$  to BSs and MS positions in general seems not possible.

We start the resolution of the ML DPE problem by maximizing with respect to  $\tilde{\sigma}^2$ . A simple computation shows that

$$\hat{\sigma}^2 = \frac{1}{MKN} \sum_{i=1}^K \sum_{n=0}^{N-1} \|\mathbf{y}_{i,n} - \tilde{\gamma}_i(\tilde{\mathbf{x}}_i^{\text{LOS}} + \tilde{\mathbf{x}}_i^{\text{NLOS}})c_{i,n}\|^2. \quad (12)$$

Substituting this value back in (11), neglecting unnecessary constant terms, and considering a monotonic transformation of the log-likelihood function, we obtain the equivalent function

$$\ell(\tilde{\mathbf{p}}_0, \tilde{\boldsymbol{\gamma}}, \tilde{\boldsymbol{\xi}}) = \sum_{i=1}^K \sum_{n=0}^{N-1} \|\mathbf{y}_{i,n} - \tilde{\gamma}_i(\tilde{\mathbf{x}}_i^{\text{LOS}} + \tilde{\mathbf{x}}_i^{\text{NLOS}})c_{i,n}\|^2 \quad (13)$$

and the ML direct position estimator reduces to

$$\hat{\mathbf{p}}_0 = \arg \min_{\tilde{\mathbf{p}}_0} \left[ \min_{\tilde{\boldsymbol{\gamma}}, \tilde{\boldsymbol{\xi}}} \ell(\tilde{\mathbf{p}}_0, \tilde{\boldsymbol{\gamma}}, \tilde{\boldsymbol{\xi}}) \right]. \quad (14)$$

Clearly, minimization of (13) with respect to a specific  $\tilde{\gamma}_i \in \mathbb{C}$  is equivalent to minimization of the term  $\sum_{n=0}^{N-1} \|\mathbf{y}_{i,n} - \tilde{\gamma}_i(\tilde{\mathbf{x}}_i^{\text{LOS}} + \tilde{\mathbf{x}}_i^{\text{NLOS}})c_{i,n}\|^2$ , which yields

$$\hat{\gamma}_i = \frac{\tilde{\mathbf{x}}_i^H \tilde{\mathbf{y}}_i}{\|\tilde{\mathbf{x}}_i\|^2 \bar{c}_i} \quad i = 1, \dots, K \quad (15)$$

where  $\tilde{\mathbf{x}}_i \stackrel{\text{def}}{=} \tilde{\mathbf{x}}_i^{\text{LOS}} + \tilde{\mathbf{x}}_i^{\text{NLOS}}$ ,  $\bar{\mathbf{y}}_i \stackrel{\text{def}}{=} \sum_{n=0}^{N-1} \mathbf{y}_{i,n} c_{i,n}^*$ , and  $\bar{c}_i \stackrel{\text{def}}{=} \sum_{n=0}^{N-1} |c_{i,n}|^2$ . Substituting back in (13) leads to

$$\ell'(\tilde{\mathbf{p}}_0, \tilde{\boldsymbol{\xi}}) = \sum_{i=1}^K \left( \bar{y}_i - \frac{\|\mathbf{P}_{\tilde{\mathbf{x}}_i} \bar{\mathbf{y}}_i\|^2}{\bar{c}_i} \right) \quad (16)$$

with  $\bar{y}_i \stackrel{\text{def}}{=} \sum_{n=0}^{N-1} \|\mathbf{y}_{i,n}\|^2$  while  $\mathbf{P}_{\tilde{\mathbf{x}}_i} = \tilde{\mathbf{x}}_i \tilde{\mathbf{x}}_i^H / \|\tilde{\mathbf{x}}_i\|^2$  denotes the projector on the one-dimensional space generated by  $\tilde{\mathbf{x}}_i$ . Interestingly, (16) is parametrized as function of the MS initial position  $\mathbf{p}_0$  and of the nuisance parameters related to the NLOS paths, that is  $\boldsymbol{\xi}$ . Keeping in mind that the value of  $\tilde{\mathbf{x}}_i^{\text{LOS}}$  is uniquely determined for each position hypothesis  $\tilde{\mathbf{p}}_0$ , the computation of  $\mathbf{P}_{\tilde{\mathbf{x}}_i}$  requires the estimation of both NLOS amplitudes ( $\beta_i^m$ s) and AOAs ( $\theta_i^m$ s). However, a direct estimation of the multipath environment from (16) is not possible in this case since, in contrast to static scenarios, the number of unknown NLOS parameters significantly increases with the observation size. To overcome this drawback, we propose to reconstruct an estimate of  $\mathbf{P}_{\tilde{\mathbf{x}}_i}$  using the following suboptimal approach:

- 1) estimation of the AOAs (both LOS and NLOS) for each observation  $i \in \mathcal{Y}$  using the smooth-MUSIC algorithm for coherent environment;
- 2) adoption of an adaptive beamforming strategy that exploits a directional response of the array towards the estimated AOAs to estimate the related amplitudes.

In the following we detail such a procedure. Spatial smoothing (SS) is an effective way to decorrelate signals for some array structures [32]. In particular, the  $M$ -element ULA is divided into  $S$  virtual overlapped subarrays with each subarray composed of  $P < M$  sensors and shifted by one with respect to the previous one<sup>3</sup>. As a result, the full array is divided into  $S = M - P + 1$  subarrays. Each set of subarray data is denoted by  $\mathbf{y}_{i,n}^{(j)}, j = 1, \dots, S$ , and contains the  $P$  components of  $\mathbf{y}_{i,n}$  from  $j$  to  $j + P - 1$ , respectively. The forward-only (FO) matrix is then obtained by using the averaged sample covariance matrix  $\hat{\mathbf{R}}_{Y_i Y_i}^{\text{F}} \in \mathbb{C}^{P \times P}$ , which is defined as

$$\hat{\mathbf{R}}_{Y_i Y_i}^{\text{F}} = \frac{1}{S} \sum_{j=1}^S \hat{\mathbf{R}}_{Y_i Y_i}^{(j)} \quad (17)$$

with  $\hat{\mathbf{R}}_{Y_i Y_i}^{(j)} = (1/N) \mathbf{Y}_i^{(j)} \mathbf{Y}_i^{(j)H}$  denoting the  $j$ -th subarray sample covariance matrix and  $\mathbf{Y}_i^{(j)} \stackrel{\text{def}}{=} [\mathbf{y}_{i,0}^{(j)} \dots \mathbf{y}_{i,N-1}^{(j)}]$ . Better, a forward-backward spatial smoothing (FBSS) can be employed to decorrelate the received signal in a stronger way; after that, a MUSIC approach can be used, referred to as smooth-MUSIC in this case [33]. More precisely, let  $\mathbf{J}$  be an exchange matrix, whose elements are zero except for ones on the antidiagonal. By exploiting the translational invariance property of  $\mathbf{a}(\theta_i)$ , i.e.,  $\mathbf{J} \mathbf{a}^*(\theta_i) = e^{-j(M-1)\omega d \sin \theta_i} \mathbf{a}(\theta_i)$ , the following forward-backward sample covariance matrix can be used in place of (17)

$$\hat{\mathbf{R}}_{Y_i Y_i}^{\text{FB}} = \frac{\hat{\mathbf{R}}_{Y_i Y_i}^{\text{F}} + \mathbf{J}(\hat{\mathbf{R}}_{Y_i Y_i}^{\text{F}})^* \mathbf{J}}{2}. \quad (18)$$

Considering without loss of generality the first subarray as the reference subarray, we denote its steering vector as  $\mathbf{a}^{(1)}(\theta_i) = [1 \ e^{j\omega d \sin \theta_i} \dots e^{j(P-1)\omega d \sin \theta_i}]^T$  and compute the smooth-MUSIC algorithm on the reduced-size vector.

For each observation  $i$ , let us denote by  $\hat{\boldsymbol{\theta}}_i = [\hat{\theta}_i^1 \dots \hat{\theta}_i^{q_i}]^T$  the estimates obtained by the described procedure, i.e.,  $\hat{\theta}_i^s, s = 1, \dots, q_i$  are the directions corresponding to the peaks of the smooth-MUSIC pseudo-spectrum. Clearly,

<sup>3</sup>Denoting with  $p$  the first sensor of  $j$ -th subarray, the first sensor belonging to the  $(j+1)$ -th subarray is at position  $p+1$ .



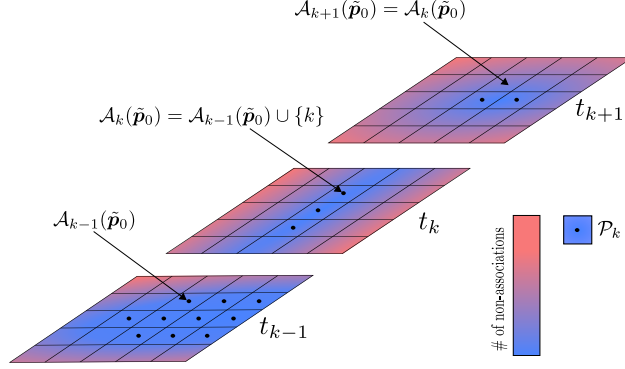


Fig. 3: Pictorial representation of a possible evolution over time for the sets  $\mathcal{A}_k$  and  $\mathcal{P}_k$ .

the number  $q_i$  of estimated components can be different from the actual  $D_i + 1$  (LOS+NLOS); nonetheless, one can expect that if there are spurious directions due to variations in the pseudo-spectrum, insignificant amplitudes will be obtained when searching through such directions. For all such  $q_i$  components, the complex amplitudes are estimated as the output of a FBSS Capon beamformer; notice that they will estimate the product of three terms:  $\beta_i^s$  — with  $s \in \{1, \dots, q_i\}$ , ideally close to one of the  $\beta_i^m$  — times  $\gamma_i$  times the array gain in the look direction. We denote by  $\hat{\alpha}_i^s$  the overall estimated amplitudes:

$$\hat{\alpha}_i^s = \mathbf{w}_{\text{FB}}^H(\hat{\theta}_i^s) \mathbf{y}_{i,n}^{(1)} \quad (19)$$

with the optimum weight vector  $\mathbf{w}_{\text{FB}} \in \mathbb{C}^{P \times 1}$  given by [34]

$$\mathbf{w}_{\text{FB}}(\hat{\theta}_i^s) = \frac{(\hat{\mathbf{R}}_{Y_i Y_i}^{\text{FB}})^{-1} \mathbf{a}^{(1)}(\hat{\theta}_i^s)}{\mathbf{a}^{(1)H}(\hat{\theta}_i^s) (\hat{\mathbf{R}}_{Y_i Y_i}^{\text{FB}})^{-1} \mathbf{a}^{(1)}(\hat{\theta}_i^s)}. \quad (20)$$

The vector of estimated amplitudes is denoted by  $\hat{\alpha}_i$ . To reconstruct a meaningful estimate of the projection matrix for the final step of the ML estimation procedure, we need to consider that also  $\beta_0$  (the component related to the LOS), although theoretically equal to 1, is estimated this way (it is one of the  $q_i$  directions). Thus, in the estimated projector all components (LOS+NLOS) share the same estimate of  $\gamma_i$ , which therefore becomes a constant that cancels out in the normalization intrinsic in  $\mathbf{P}_{\hat{\mathbf{x}}_i} = \tilde{\mathbf{x}}_i \tilde{\mathbf{x}}_i^H / \|\tilde{\mathbf{x}}_i\|^2$ . Thus, up to (minor) errors due to the array gain not being perfectly equal to 1 in the look direction — to the extent of the angle estimation errors from the smooth-MUSIC — the projection matrix can be reconstructed. To this aim, the main problem remains the identification of the LOS, i.e., the association of one of the estimated directions  $\hat{\theta}_i^s$  to the direct path, in order to separate the complementary NLOS components involved in  $\mathbf{P}_{\hat{\mathbf{x}}_i}$  from the LOS component that is coherently processed over the whole trajectory for  $i = 1, \dots, K$ . We proceed as follows.

- For each trial position  $\tilde{\mathbf{p}}_0$  in a grid, and based on the trajectory resulting from the velocity measurements up to time  $t_i$ , we can reconstruct the trial LOS angle  $\tilde{\theta}_i^{\text{LOS}}$ .
- This direction is compared against the estimated AOAs at  $i$ : if a  $\hat{\theta}_i^*$  in  $\hat{\theta}_i$  is found such that its distance to  $\tilde{\theta}_i^{\text{LOS}}$  is less than a tolerance  $\delta$  (namely, a few degrees), then  $\hat{\theta}_i^*$  is associated to the LOS; as a consequence, its

estimated amplitude  $\hat{\alpha}_i^*$  (taken from  $\hat{\alpha}_i$ ) is used to compute an estimate of the LOS signal  $\hat{\mathbf{x}}_i^{\text{LOS}} = \hat{\alpha}_i^* \mathbf{a}(\tilde{\theta}_i^{\text{LOS}})$  — notice that  $\tilde{\theta}_i^{\text{LOS}}$  is used in the reconstruction, not  $\hat{\theta}_i^*$ .

- Likewise, we compute an estimate of the NLOS signal as  $\hat{\mathbf{x}}_i^{\text{NLOS}} = \sum_j \hat{\alpha}_j^{\text{NLOS}} \mathbf{a}(\hat{\theta}_j^{\text{NLOS}})$  with  $\hat{\alpha}_j^{\text{NLOS}} \in \hat{\alpha}_i \setminus \{\hat{\alpha}_i^*\}$  and  $\hat{\theta}_j^{\text{NLOS}} \in \hat{\theta}_i \setminus \{\hat{\theta}_i^*\}$ . This yields an estimate of the projector over  $\hat{\mathbf{x}}_i = \hat{\mathbf{x}}_i^{\text{LOS}} + \hat{\mathbf{x}}_i^{\text{NLOS}}$ , i.e.,  $\hat{\mathbf{P}}_{\hat{\mathbf{x}}_i}$ , to be used in the final optimization of the (compressed) likelihood function, i.e.,

$$\hat{\mathbf{p}}_0 = \arg \max_{\tilde{\mathbf{p}}_0 \in \mathcal{P}} \sum_{i \in \mathcal{A}(\tilde{\mathbf{p}}_0)} \frac{\|\hat{\mathbf{P}}_{\hat{\mathbf{x}}_i}(\tilde{\mathbf{p}}_0) \bar{\mathbf{y}}_i\|^2}{\bar{c}_i} \quad (21)$$

where we have remarked the dependency of the projection matrix on  $\tilde{\mathbf{p}}_0$ .

Notice that in (21) the sum is taken on the subset  $\mathcal{A}(\tilde{\mathbf{p}}_0)$  of indexes for which the LOS association has been performed. In fact, if in  $\hat{\theta}_i$  there is no estimated direction sufficiently close to the coherent LOS trajectory under evaluation, obtained from a given trial point  $\tilde{\mathbf{p}}_0$ , such  $i$ -th term is discarded from the cost function. The algorithm will keep state of the number of indexes not associated (i.e., terms discarded in the cost function) for each trial point  $\tilde{\mathbf{p}}_0$  in the grid; once the evaluation of all points is concluded, the maximum will be taken only on the subset  $\mathcal{P}$  of grid points with minimum number of non-associations, since the likelihood of LOS association is maximized for points close to the true one. Fig. 2 illustrates this idea by showing two examples of reconstructed trajectories based on different  $\tilde{\mathbf{p}}_0$ , in comparison with the true trajectory (black curve in the middle). Clearly, all ordered segments of the reconstructed trajectories are parallel to each other since they use the same velocity estimates  $(\mathbf{v}(t_0), \mathbf{v}(t_1), \dots)$ , with some misalignment compared to the true trajectory due to the measurement errors. Thus, it is expected that a  $\tilde{\mathbf{p}}_0$  closer to the true  $\mathbf{p}_0$  will produce a smaller value in the cost function.

To further clarify, Fig. 3 depicts an example of possible evolution over time for the set  $\mathcal{P}$ . The algorithm can be implemented in an on-line fashion since the association decision for past observations does not change over time. In particular, denoting by  $\mathcal{P}_k$  the subset of grid points with minimum number of non-associations at time  $k$ , eq. (21) can be rewritten in a recursive form as follows

$$\hat{\mathbf{p}}_0(k) = \arg \max_{\tilde{\mathbf{p}}_0 \in \mathcal{P}_k} S_k(\tilde{\mathbf{p}}_0) \quad (22)$$

where

$$S_k(\tilde{\mathbf{p}}_0) = S_{k-1}(\tilde{\mathbf{p}}_0) + \delta_k(\tilde{\mathbf{p}}_0) \frac{\|\hat{\mathbf{P}}_{\hat{\mathbf{x}}_k} \bar{\mathbf{y}}_k\|^2}{\bar{c}_k}$$

with

$$S_{k-1}(\tilde{\mathbf{p}}_0) = \sum_{i \in \mathcal{A}_{k-1}(\tilde{\mathbf{p}}_0)} \frac{\|\hat{\mathbf{P}}_{\hat{\mathbf{x}}_i} \bar{\mathbf{y}}_i\|^2}{\bar{c}_i},$$

$$\delta_k(\tilde{\mathbf{p}}_0) = \begin{cases} 1 & \text{if } k\text{-th meas. associated to LOS given } \tilde{\mathbf{p}}_0 \\ 0 & \text{otherwise} \end{cases}$$

and

$$\mathcal{A}_k(\tilde{\mathbf{p}}_0) = \begin{cases} \mathcal{A}_{k-1}(\tilde{\mathbf{p}}_0) \cup \{k\} & \text{if } \delta_k(\tilde{\mathbf{p}}_0) = 1 \\ \mathcal{A}_{k-1}(\tilde{\mathbf{p}}_0) & \text{otherwise} \end{cases}.$$

As a final remark, we observe that the proposed algorithm intrinsically handles transmissions from multiple BS, “interleaved” in the time index  $i$  (according to the arrival time) without any additional complexity. It is only sufficient to consider for each transmission the appropriate BS position.

For the sake of clarity, the algorithm steps are summarized in Algorithm 1. Notice that, despite the algorithmic procedure is articulated in several steps, the computational complexity is limited thanks to the recursive implementation.

### B. Max-power beamformer based DPE

As a simpler alternative to the algorithm above, an ad-hoc solution can be obtained by considering the expected power at the output of the beamformer. In particular, the idea is to use a compressed version of the observations  $\mathcal{Y}$ , namely  $\mathcal{Z} = \{z_1(\theta_1), \dots, z_K(\theta_K)\}$  with  $z_i(\theta_i) = (\mathbf{w}_{\text{FB}}^H(\theta_i) \mathbf{Y}_i^{(1)})^T$ , which are parameterized as function of the look angles  $\{\theta_1, \dots, \theta_K\}$  (we stress the dependencies on  $\theta_i$ ) and with the optimum weight vector  $\mathbf{w}_{\text{FB}} \in \mathbb{C}^{P \times 1}$  given by

$$\mathbf{w}_{\text{FB}}(\theta_i) = \frac{(\hat{\mathbf{R}}_{Y_i Y_i}^{\text{FB}})^{-1} \mathbf{a}^{(1)}(\theta_i)}{\mathbf{a}^{(1)H}(\theta_i) (\hat{\mathbf{R}}_{Y_i Y_i}^{\text{FB}})^{-1} \mathbf{a}^{(1)}(\theta_i)}. \quad (23)$$

More precisely, for a given position trial  $\tilde{\mathbf{p}}_0$ , each look angle  $\tilde{\theta}_i$  is determined by computing  $\tilde{\mathbf{p}}(t_i)$  through (8), followed by the application of (7). This leads to

$$\hat{\mathbf{p}}_0 = \arg \max_{\tilde{\mathbf{p}}_0} \sum_{i=1}^K \|\mathbf{z}_i(\tilde{\theta}_i)\|^2. \quad (24)$$

Such a DPE algorithm is completely different and does not exploit the knowledge of the symbols  $c_{i,n}$ . Intuitively, it aims at measuring the amount of energy collected over time for each trial position  $\tilde{\mathbf{p}}_0$ . In so doing, when  $\tilde{\mathbf{p}}_0 \approx \mathbf{p}_0$ , the look directions would be close to the actual  $\{\theta_1^{\text{LOS}}, \dots, \theta_K^{\text{LOS}}\}$  and the cumulative energy will take into account the contributions of LOS paths, which contain considerably higher power than that of all the NLOS components. However, since only a finite number of noisy samples is available, we expect that the estimated energy may exhibit significant deviations from its actual value, especially when a high number of NLOS components is present (dense multipath).

For the sake of clarity, the algorithm steps are summarized in Algorithm 2. Notice that the computational complexity is lower than Algorithm 1; as will be shown in the analysis below, this is in trade-off with the localization performance, especially in dense multipath conditions.

### C. Single-path ML DPE

For comparison purposes, in this section we derive a single-path (SP) ML DPE algorithm that ignores the NLOS components. Notice that this is tantamount to considering that all multipath effects are modeled as additive white Gaussian noise, as done in [15], [16]. However, we cannot directly take [15], [16] as competitors since they are for stationary, not mobile nodes. For a fair comparison we thus merge the ML localization approach for mobile nodes proposed in this paper with the statistical characterization of a SP approach, that is, the received signals characterization (9) is approximated as

$$\mathbf{y}_{i,n} \sim \mathcal{CN}_M(\gamma_i \mathbf{x}_i^{\text{LOS}} c_{i,n}, \sigma_{\text{sp}}^2 \mathbf{I}_M) \quad (25)$$

---

**Algorithm 1** ML-based DPE (online implementation)

---

```

1: Initialize:
2: Set  $k = 0$ ,  $\mathcal{P}_0 = \{(x, y) \text{ of a chosen 2D grid}\}$ 
3: for each  $\tilde{\mathbf{p}}_0 \in \mathcal{P}_0$  do
4:    $\mathcal{A}_0(\tilde{\mathbf{p}}_0) = \{\emptyset\}$ 
5:    $S_0(\tilde{\mathbf{p}}_0) = 0$ 
6:    $I(\tilde{\mathbf{p}}_0) = 0$ 
7: end for
8: loop
9:   New observation:  $k \leftarrow k + 1$  (process  $\mathbf{Y}_k$  at  $t_k$ )
10:  Compute  $\hat{\boldsymbol{\theta}}_k$  using the smooth-MUSIC algorithm
11:  for each  $\hat{\theta}_k^s$  in  $\hat{\boldsymbol{\theta}}_k$  do
12:    Compute beamformer weights  $\mathbf{w}_{\text{FB}}(\hat{\theta}_k^s)$  using (20)
13:    Compute  $\hat{\alpha}_k^s$  using (19)
14:  end for
15:  for each  $\tilde{\mathbf{p}}_0 \in \mathcal{P}_0$  do
16:    Compute  $\tilde{\theta}_k^{\text{LOS}}$  using (7) and (8)
17:    for each  $\hat{\theta}_k^s$  in  $\hat{\boldsymbol{\theta}}_k$  do
18:      Compute  $d_k^s = |\tilde{\theta}_k^{\text{LOS}} - \hat{\theta}_k^s|$ 
19:    end for
20:    if  $\min_{s=1, \dots, q_k} \{d_k^s\} \leq \delta$  then
21:      Compute  $\hat{\mathbf{P}}_{\tilde{\mathbf{x}}_k}(\tilde{\mathbf{p}}_0)$ 
22:      Compute  $S_k(\tilde{\mathbf{p}}_0) = S_{k-1}(\tilde{\mathbf{p}}_0) + \frac{\|\hat{\mathbf{P}}_{\tilde{\mathbf{x}}_k} \mathbf{y}_k\|^2}{\tilde{c}_k}$ 
23:      Update  $\mathcal{A}_k(\tilde{\mathbf{p}}_0) = \mathcal{A}_{k-1}(\tilde{\mathbf{p}}_0) \cup \{k\}$ 
24:    else
25:       $I(\tilde{\mathbf{p}}_0) \leftarrow I(\tilde{\mathbf{p}}_0) + 1$ 
26:    end if
27:  end for
28:   $\mathcal{P}_k = \{\tilde{\mathbf{p}}_0 \in \mathcal{P}_0 \text{ s.t. } I(\tilde{\mathbf{p}}_0) = \min I\}$ 
29:  Compute  $\hat{\mathbf{p}}_0(k) = \arg \max_{\tilde{\mathbf{p}}_0 \in \mathcal{P}_k} S_k(\tilde{\mathbf{p}}_0)$ 
30:  Reconstruct  $\hat{\mathbf{p}}(t_k)$  using (8)
31: end loop

```

---

---

**Algorithm 2** Max-power beamformer based DPE
 

---

```

1: Initialize:
2: Set  $k = 0$ ,  $\mathcal{P}_0 = \{(x, y) \text{ of a chosen 2D grid}\}$ 
3: for each  $\tilde{\mathbf{p}}_0 \in \mathcal{P}_0$  do
4:    $S_0(\tilde{\mathbf{p}}_0) = 0$ 
5: end for
6: loop
7:   New observation:  $k \leftarrow k + 1$  (process  $\mathbf{Y}_k$  at  $t_k$ )
8:   Compute  $\tilde{\theta}_k$  using (7) and (8)
9:   Compute beamformer weights  $\mathbf{w}_{\text{FB}}(\tilde{\theta}_k)$  using (23)
10:  Compute  $\mathbf{z}_k(\tilde{\theta}_k) = (\mathbf{w}_{\text{FB}}^H(\tilde{\theta}_k) \mathbf{Y}_k^{(1)})^T$ 
11:  for each  $\tilde{\mathbf{p}}_0 \in \mathcal{P}_0$  do
12:    Compute  $S_k(\tilde{\mathbf{p}}_0) = S_{k-1}(\tilde{\mathbf{p}}_0) + \|\mathbf{z}_k(\tilde{\theta}_k)\|^2$ 
13:  end for
14:  Compute  $\hat{\mathbf{p}}_0(k) = \arg \max_{\tilde{\mathbf{p}}_0 \in \mathcal{P}_0} S_k(\tilde{\mathbf{p}}_0)$ 
15:  Reconstruct  $\hat{\mathbf{p}}(t_k)$  using (8)
16: end loop

```

---

where  $\sigma_{\text{sp}}^2$  denotes the ultimate variance accounting for both thermal noise and NLOS contributions, and  $\mathbf{x}_i^{\text{LOS}} = \mathbf{a}(\theta_i^{\text{LOS}})$  as usual. In this case the log-likelihood function is expressed as

$$L(\tilde{\mathbf{p}}_0, \sigma_{\text{sp}}^2, \tilde{\gamma}) = - \left[ MKN \log(\pi \sigma_{\text{sp}}^2) + \frac{1}{\sigma_{\text{sp}}^2} \sum_{i=1}^K \sum_{n=0}^{N-1} \|\mathbf{y}_{i,n} - \tilde{\gamma}_i \mathbf{a}(\tilde{\theta}_i) c_{i,n}\|^2 \right] \quad (26)$$

where, again, for a given position trial  $\tilde{\mathbf{p}}_0$  the resulting trial LOS directions  $\tilde{\theta}_i, i = 1, \dots, K$ , are obtained from the application of (8) and (7). The maximum of (26) with respect to  $\sigma_{\text{sp}}^2$  is given by

$$\hat{\sigma}_{\text{sp}}^2 = \frac{1}{MKN} \sum_{i=1}^K \sum_{n=0}^{N-1} \|\mathbf{y}_{i,n} - \tilde{\gamma}_i \mathbf{a}(\tilde{\theta}_i) c_{i,n}\|^2. \quad (27)$$

Substituting this expression back in (26), neglecting unnecessary constant terms, and considering a monotonic transformation of the log-likelihood, we obtain

$$\ell_{\text{sp}}(\tilde{\mathbf{p}}_0, \tilde{\gamma}) = \sum_{i=1}^K \sum_{n=0}^{N-1} \|\mathbf{y}_{i,n} - \tilde{\gamma}_i \mathbf{a}(\tilde{\theta}_i) c_{i,n}\|^2. \quad (28)$$

It is a simple matter to show that maximization of (28) with respect to a specific  $\tilde{\gamma}_i \in \mathbb{C}$  is solved by

$$\hat{\gamma}_i = \frac{\sum_{n=0}^{N-1} |\mathbf{a}^H(\tilde{\theta}_i) \mathbf{y}_{i,n} c_{i,n}^*|^2}{\sum_{n=0}^{N-1} \|\mathbf{a}(\tilde{\theta}_i) c_{i,n}\|^2} \quad i = 1, \dots, K. \quad (29)$$

Substituting these maximizing values back in (28), the final ML DPE is obtained as

$$\hat{\mathbf{p}}_0 = \arg \min_{\tilde{\mathbf{p}}_0} \sum_{i=1}^K \sum_{n=0}^{N-1} \|\mathbf{y}_{i,n} - \hat{\gamma}_i \mathbf{a}(\tilde{\theta}_i) c_{i,n}\|^2. \quad (30)$$

#### IV. SIMULATION MODEL AND RESULTS

In this section, we analyze the performance of the proposed algorithms by means of simulations. We consider a MS equipped with a  $M = 64$  element ULA, running the proposed localization algorithms, and different test scenarios with one or more BSs that broadcast signals with a rate  $R_{BS} = 10$  Hz. To simulate a realistic environment, we model several phenomena and non idealities that can be found in real contexts. It is worth remarking, thus, that the performance assessment is carried out in a simulation environment that is not matched to the design assumptions of the proposed algorithms. We consider the root mean squared error (RMSE) as performance metric, estimated based on 1000 Monte Carlo trials.

##### A. Simulation model

In the following, we give a detailed description of the models adopted for the simulation.

1) *Mobility model*: We assume that the MS follows a linear trajectory along the  $y$  direction, with a velocity profile characterized by a uniform acceleration starting from 25 km/h up to 50 km/h for one third of the path, followed by a constant velocity motion at 50 km/h for the second third, and ended with a deceleration until reaching the initial speed of 25 km/h, resulting in a total path of 8 seconds. MS velocity measurement errors are modeled as independent Gaussian variables with zero mean and standard deviations equal to 10% of the true value of the velocities.

2) *Channel model*: We assume a carrier frequency  $f_c = 5.9$  GHz and a transmit power  $P_{T,dB} = 18$  dBm<sup>4</sup>. The wireless propagation is modeled according to [29]; in particular, the path loss at distance  $d$  from the transmitter is obtained by the well-known formula

$$L_{PL,dB} = 10\eta \log_{10} \frac{d}{d_0} \quad (31)$$

with path loss exponent  $\eta = 4$  and  $d_0 = 1$  m the reference distance. According to the experimental campaign conducted in [35], we set the channel parameters  $B_c = 250$  kHz and  $B_D = 512$  Hz, which represent a harsh multipath environment.

Following the Clarke's model [36] for a MS moving in dense multipath environments, we assume that the NLOS contributions can arrive at the receiver from all directions, uniformly distributed in the space, i.e.,  $\theta_i^m \sim \mathcal{U}(0, 2\pi)$ . Each complex multipath coefficient can be expressed in terms of  $\beta_i^m = a_i^m e^{j\varphi_i^m}$  with  $a_i^m$  the amplitude of the  $m$ -th NLOS component and  $\varphi_i^m = 2\pi f_c \tau_i^m$  the phase shift related to the time delay  $\tau_i^m$ , respectively. Following [29], we model  $\varphi_i^m \sim \mathcal{U}(0, 2\pi)$ , while the multipath amplitude  $a_i^m$  is chosen according to a deterministic power delay profile (PDP)  $P(\tau_i^m)$ , which accounts for the propagation loss as function of the time delay  $\tau_i^m$ . In this work, we have chosen  $P(\tau_i^m)$  as an exponential decaying function of  $\tau_i^m$ , i.e.

$$P(\tau_i^m) = e^{-\tau_i^m / \sigma_\tau} \quad (32)$$

with  $\sigma_\tau = 677$  ns denoting the channel RMS delay spread, set according to [35].

<sup>4</sup>Such values are typical of mobile communications based e.g. on the IEEE 802.11p standard.

To take into account severe LOS obstructions, 10% of the links are randomly assigned to the NLOS class, while we recall that all algorithms assume there is always a direct path. As for the symbols, we assume a QPSK constellation for generating the random sequence  $c_{i,n}$ ,  $i = 1, \dots, K$ ,  $n = 0, \dots, N - 1$ .

3) *System parameters*: We set the observation period  $T_{obs} = T_c = 325 \mu s$ , with  $T_c$  the channel coherence time obtained from the assumed Doppler spread  $B_D^5$ . As a consequence, the number of finite samples that can be collected for each observation is  $N = 16$ , which corresponds to a signal bandwidth  $B$  from 25 to 50 kHz according to the choice of the roll-off factor  $\alpha_{\text{RRCR}}$ . In Appendix we report the exact computation of such values, which shows the existence of system parameter settings such that all the assumptions given before (1) (*flat* and *slow* fading) are jointly satisfied.

4) *Competitors*: As concerns the competitors, we consider the SP ML algorithm — which we recall can be considered as an extension of [15], [16] to the mobile case, for a fair comparison — and we implemented a modified version of the WLS proposed in [3], which is an indirect position estimator (IPE). More precisely, we replaced the MUSIC algorithm (inapplicable here) with the smooth-MUSIC, followed by the application of the beamforming to estimate the LOS direction as the angle associated with the strongest output power.

#### B. Localization based on single Base Station

The first analyzed scenario is a minimal situation involving only the MS and a single BS initially distant 60 m. The MS moves towards the BS and crosses it after about 5.25 s, as shown in Fig. 4a. The RMSEs of the MS position estimates for the different algorithms in the case  $D_i = 10$  are reported in Fig. 4b (solid lines). As it can be seen, the ML-based DPE algorithm initially exhibits a relatively high error, which however immediately starts to decrease as more measurements are available. Interestingly, the RMSE abruptly drops between 4 and 5 s, exhibiting values below one meter and thus outperforming all the other methods. In fact, the proposed ML-based DPE algorithm is able to consistently exploit the additional information progressively available to correctly identify the most probable initial position  $\tilde{\mathbf{p}}_0$ , thanks to a more and more accurate reconstruction of the unknown optimal projector  $\mathbf{P}_{\mathbf{x}_i}$ . Notice that the performance are still remarkable also for the challenging case  $D_i = 25$  (dashed lines with markers), with only a slightly longer settling time.

The localization capability of the simpler Max-power DPE algorithm is also interesting, at least for non-severe multipath conditions. More precisely, we can observe that the RMSE tends to decrease as the MS approaches the BS (except for the short period corresponding to AOAs close to 90 degrees), stabilizing around values of error close to 2 or 3 m, depending on the multipath level. From this behavior it can be deduced that, as long as the multipath environment is not severe, the Max-power DPE can be a valid simpler alternative to the ML-based DPE. Conversely, the single-path ML-based algorithm exhibits unsatisfactory performance, meaning that the effects of multipath cannot be neglected in the considered scenario.

As regards the competitor WLS IPE, the results clearly show that its performance is totally unacceptable even under milder multipath conditions with a gap of more than 600% compared to the proposed ML-based DPE. This

<sup>5</sup>We recall that the Doppler spread  $B_D$  and coherence time  $T_c$  are inversely proportional to one another (see [29]).

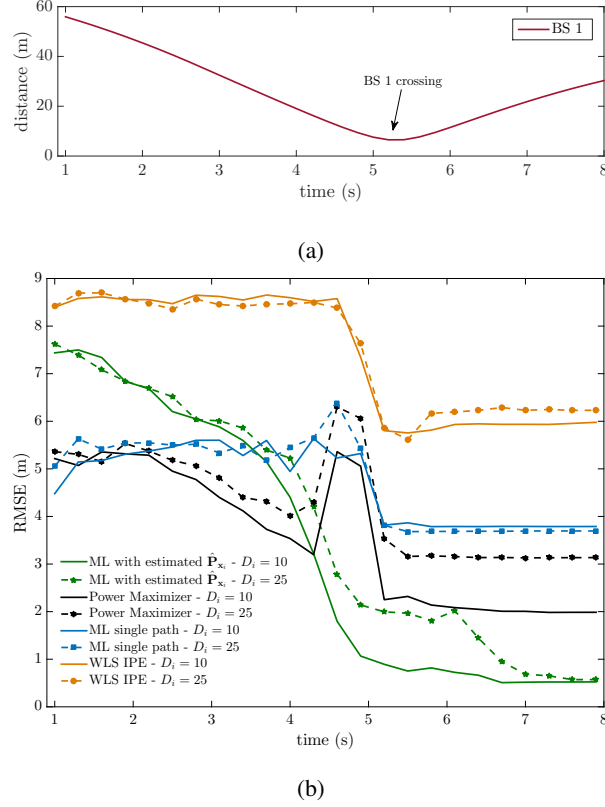


Fig. 4: (a) Distance between the MS and a single BS as function of the time. (b) RMSEs of the algorithms for the case of  $D_i = 10$  in comparison with the performance obtained for  $D_i = 25$ .

result is in agreement with the generally worse performance of IPE approaches compared to DPE ones, already observed in the literature (as discussed in Sec. I).

### C. Localization based on multiple Base Stations

When more BSs are available in range, the performance generally improve but, remarkably, the gain for the proposed ML-based DPE is dramatic. Indeed, by considering just two BSs instead of one (in particular, one BS is still at 60 m while a second one is at 20 m) the RMSE immediately drops to sub-meter accuracy, also for severe multipath conditions, as shown in Fig. 5b. Conversely, for  $D_i = 25$  the single-path ML-based and Max-power algorithms show almost flat performance over time, meaning that, due to the dense multipath, they are not able to take advantage of the additional information collected during the motion. It is though worth noticing that for  $D_i = 10$  the Max-power algorithm has quite good performance, although it requires a large number of measurements to attain 1-meter accuracy.

To conclude the analysis, we show the performance of the algorithms when the minimal value for the number of antennas  $M$  is considered. Specifically, given a value of  $D_i$ , we recall that the theoretical minimum number



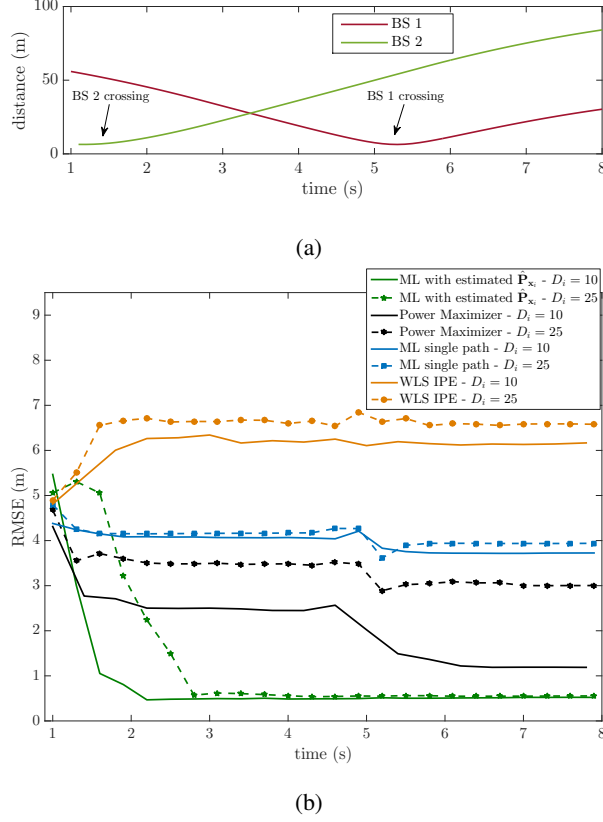


Fig. 5: (a) Distance between the MS and two BSs as function of the time. (b) RMSEs of the algorithms for the case of  $D_i = 10$  in comparison with the performance obtained for  $D_i = 25$ .

of antennas to make the problem well-posed is obtained considering  $S = (D_i + 1)/2$  subarrays, each of length  $P = D_i + 1$  [34]; this leads to  $M = 16$  and  $M = 38$  for  $D_i = 10$  and  $D_i = 25$ , respectively. The obtained results are reported in Fig. 6. Remarkably, the proposed ML-based DPE algorithm still exhibits the best performance. Again, for dense multipath, the RMSE of the competitors has a floor due to the fact that such algorithms are not able to get rid of the interfering NLOS paths.

## V. CONCLUSION

In this work, we have designed a low complexity and fully adaptive DPE algorithm for localizing a mobile node in presence of dense multipath. Our solution is based on the ML approach and exploits the training sequence of a narrowband radio signal. The algorithm employs an adaptive beamforming technique to reconstruct an estimate of the optimal projection matrix, which is then used to project the received signal over a subspace orthogonal to the multipath. Furthermore, it takes advantage of a simple and effective LOS association method to identify the most probable MS initial position, hence achieving an integration gain over time. A simpler alternative which maximizes the expected power at the output of the beamformer is also provided. The performance assessment has been

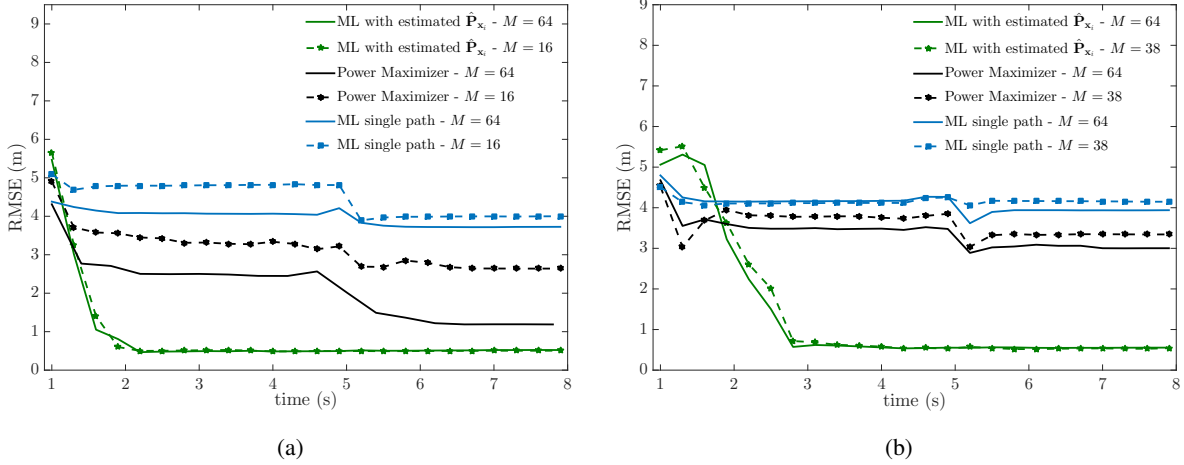


Fig. 6: (a) RMSEs of the algorithms for the case  $D_i = 10$  and for both  $M = 64$  and  $M = 16$ . (b) RMSEs of the algorithms for the case of  $D_i = 25$  and for both  $M = 64$  and  $M = 38$ .

conducted by means of simulations considering realistic values of kinematic, communication, and environmental parameters. The obtained results revealed that the proposed algorithms are very effective even in presence of few BSs and dense multipath, significantly outperforming state-of-the-art competitors.

#### APPENDIX

In this section, we conduct an analysis aimed at determining a possible choice of the system parameters  $T_{obs}$  and  $B$  such that all the assumptions before (1) are jointly satisfied.

We first analyze the MS mobility to identify a time interval, referred to as  $T_{sta}$ , in which it is possible to reasonably assume that the multipath environment remains practically unchanged. By constraining the variation of the steering vector  $\mathbf{a}(\theta_i^{LOS})$  to be lower than a predefined threshold  $\kappa$  over a finite interval  $[t_i, t_i + \Delta T]$ , we obtain

$$T_{sta} = \max \Delta T$$

$$s.t. \quad \|\mathbf{a}(\theta_i^{LOS}) - \mathbf{a}(\theta_{i+\Delta T}^{LOS})\| \leq \kappa \quad (33)$$

where  $\theta_{i+\Delta T}^{LOS}$  is readily determined from the computation of  $\mathbf{p}(t_{i+\Delta T})$  through (8), followed by the application of the geometric model in (7). We consider a linear trajectory at a constant velocity of 50 km/h, which is the maximum speed considered in the simulations hence represents a conservative choice. Solving the constrained problem in (33) for  $\kappa = 0.01$  allows us to determine the value of  $T_{sta}$  such that the maximum variation of  $\mathbf{a}(\theta_i^{LOS})$  due to MS mobility does not exceed 1%, i.e., it is practically negligible. Notice that the entity of the variation strictly depends on the nonlinear relation between  $\mathbf{p}(t_i)$  and  $\theta_i^{LOS}$ , as given in (7). Therefore, two different cases have been analyzed: i) the MS is 100 m far from the BS; ii) the MS is 20 m far from the BS. The resulting value of  $T_{sta}$  is 122 ms in the first case and 6 ms in the second case, respectively. As it can be noticed, the variation is much higher for closer distances, as direct consequence of the nonlinear increase of  $\theta_i^{LOS}$  as the MS approaches the BS. However,

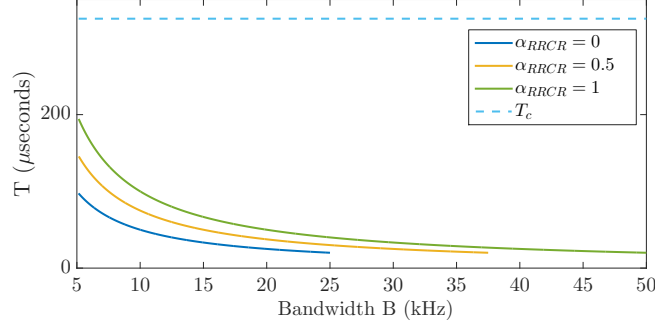


Fig. 7: Sampling interval  $T$  as function of the bandwidth  $B$  for three different values of the roll-off factor  $\alpha_{\text{RRCR}}$ .

the values of  $T_{sta}$  are significantly greater than the channel coherence time  $T_c$ , meaning that this latter represents the most stringent constraint.

By jointly considering all the assumptions discussed in Sec. II, we obtain the following set of constraints

$$\begin{cases} T_{obs} \leq T_c \\ B \gg B_D \\ B \ll B_c(1 + \alpha_{\text{RRCR}}) \end{cases} \quad (34)$$

In Fig. 7 we draw the values of the sampling interval  $T$  as function of the bandwidth  $B$  satisfying all the conditions in (34). As it can be observed,  $T$  is much lower than the channel coherence time  $T_c$  for all the possible values of roll-off  $\alpha_{\text{RRCR}}$ . Moreover, it should be noticed that different values of  $\alpha_{\text{RRCR}}$  give rise to different ranges of allowed  $B$ , as shown by the three solid curves. Interestingly, all the three hyperbolas attain the same minimum value of  $T$ , leading to the same number of collected samples  $N = \lfloor \frac{T_{obs}}{T} \rfloor = 16$ , but for different bandwidths  $B$ . Thus, standing the same value of  $N$ , one can consider the most convenient choice of  $\alpha_{\text{RRCR}}$  based on practical considerations regarding bandwidth consumption and ease of electronic implementation of the pulse shaper.

## REFERENCES

- [1] N. Patwari, J. Ash, S. Kyperountas, A. O. Hero, III, R. Moses, and N. Correal: "Locating the nodes: Cooperative localization in wireless sensor networks," *IEEE Signal Process. Mag.*, Vol. 22, No. 4, pp. 54–69, June 2005.
- [2] S. Tomic, M. Beko, R. Dinis, and P. Montezuma: "Distributed Algorithm for Target Localization in Wireless Sensor Networks Using RSS and AoA Measurements," *Pervasive Mobile Comput.*, Vol. 37, pp. 63–77, June 2017.
- [3] A. Fascista, G. Ciccarese, A. Coluccia, and G. Ricci: "A Localization Algorithm Based on V2I Communications and AOA Estimation," *IEEE Signal Process. Lett.*, Vol. 24, No. 1, pp 136–140, Jan. 2017.
- [4] S. Tomic, M. Beko, R. Dinis, and P. Montezuma: "A Closed-form Solution for RSS/AoA Target Localization by Spherical Coordinates Conversion," *IEEE Wireless Commun. Lett.*, Vol. 5, No. 6, pp. 680–683, Dec. 2016.
- [5] K. Cheung, H. So, W. K. Ma, and Y. Chan: "Least squares algorithms for time-of-arrival-based mobile location," *IEEE Trans. on Signal Process.*, Vol. 52, No. 4, pp. 1121–1130, April 2004.
- [6] A. Savvides, C. C. Han, and M. B. Strivastava: "Dynamic fine-grained localization in ad-hoc networks of sensors," *Proc. ACM Int. Conf. Mobile Computing Networking (MOBICOM)*, Rome, pp. 166–179, July 2001.
- [7] Y. Huang, J. Benesty, G. Elko, and R. Mersereati: "Real-time passive source localization: A practical linear-correction least-squares approach," *IEEE Trans. Speech and Audio Process.*, Vol. 9, No. 8, pp. 943–956, Nov. 2001.
- [8] A. Shahmansoori, G. E. Garcia, G. Destino, G. Seco-Granados, and H. Wymeersch: "Position and Orientation Estimation Through Millimeter-Wave MIMO in 5G Systems," *IEEE Trans. on Wireless Commun.*, Vol. 17, No. 3, pp. 1822–1835, March 2018.

- [9] T. S. Rappaport, G. R. MacCartney, M. K. Samimi, and S. Sun: "Wideband Millimeter-Wave Propagation Measurements and Channel Models for Future Wireless Communication System Design," *IEEE Trans. on Commun.*, Vol. 63, No. 9, pp. 3029–3056, Sept. 2015.
- [10] A. Fascista, G. Ciccarese, A. Coluccia, and G. Ricci: "Angle of Arrival- Based Cooperative Positioning for Smart Vehicles," *IEEE Trans. on Intelligent Transportation Systems*, Vol. PP, No. 99, pp. 1–13, 2017.
- [11] A. Coluccia and F. Ricciato: "RSS-based localization via Bayesian ranging and Iterative Least Squares positioning," *IEEE Commun. Lett.*, Vol. 18, No. 5, pp. 873–876, May 2014.
- [12] A. Coluccia: "Reduced-Bias ML-Based Estimators with Low Complexity for Self-Calibrating RSS Ranging," *IEEE Trans. on Wireless Commun.*, Vol. 12, No. 3, pp. 1220–1230, Mar. 2013.
- [13] P. Closas, C. Fernandez-Prades, and J. A. Fernandez-Rubio: "Direct Position Estimation approach outperforms conventional two-steps positioning," *IEEE Proc. Eur. Signal Process. Conf. (EUSIPCO)*, Glasgow, pp. 1958–1962, Aug. 2009.
- [14] A. Amar and A. J. Weiss: "Direct position determination in the presence of model errors - Known waveforms," *Digital Signal Process. (DSP)*, Vol. 16, No.1, pp. 52–83, Jan. 2006.
- [15] A. J. Weiss: "Direct position determination of narrowband radio frequency transmitters," *IEEE Signal Process. Lett.*, Vol. 11, No. 5, pp. 513–516, May 2004.
- [16] P. Closas, C. Fernandez-Prades, and J. A. Fernandez-Rubio: "Maximum likelihood estimation of position in GNSS," *IEEE Signal Process. Lett.*, Vol. 14, No. 5, pp. 359–362, May 2007.
- [17] A. Amar and A. J. Weiss: "Direct Position Determination of Multiple Radio Signals," *IEEE Proc. Int. Conf. Acoust., Speech, Signal Process. (ICASSP)*, Montreal, Vol. 2, pp. 81–84, May 2004.
- [18] T. Tirer and A. J. Weiss: "High Resolution Direct Position Determination of Radio Frequency Sources," *IEEE Signal Process. Lett.*, Vol. 23, No. 2, pp. 192–196, Feb. 2016.
- [19] L. Tzafrir and A. J. Weiss: "High-Resolution Direct Position Determination Using MVDR," *IEEE Trans. on Wireless Commun.*, Vol. 15, No. 9, pp. 6449–6461, Sept. 2016.
- [20] O. Bar-Shalom and A. J. Weiss: "Efficient direct position determination of orthogonal frequency division multiplexing signals," *IET Radar, Sonar & Navigation*, Vol. 3, No. 2, pp. 101–111, April 2009.
- [21] A.M. Reuven and A. J. Weiss: "Direct position determination of cyclostationary signals," *Signal Process.*, Vol. 89, No. 12, pp. 2448–2464, Dec. 2009.
- [22] M. Oispuu and U. Nickel: "Direct detection and position determination of multiple sources with intermittent emission," *Signal Process.*, Vol. 90, No. 12, pp. 3056–3064, Dec. 2010.
- [23] J. C. Chen, R. E. Hudson, and Kung Yao: "Maximum-likelihood source localization and unknown sensor location estimation for wideband signals in the near-field," *IEEE Trans. on Signal Process.*, Vol. 50, No. 8, pp. 1843–1854, Aug. 2002.
- [24] O. Bialer, D. Raphaeli, and A. J. Weiss: "Maximum-likelihood direct position estimation in dense multipath," *IEEE Trans. Veh. Technol.*, Vol. 62, No. 5, pp. 2069–2079, Aug. 2013.
- [25] N. Garcia, A. M. Haimovic, M. Coulon, and A. J. Dabin: "High precision TOA-based direct localization of multiple sources in multipath," *arXiv:1505.03193*, May 2015.
- [26] K. Papakonstantinou and D. Slock: "Direct location estimation using single-bounce NLOS time-varying channel models," *IEEE Veh. Techn. Conf. (VTC)*, Calgary, pp. 1–5, Sept. 2008.
- [27] N. Garcia, H. Wymeersch, E. G. Larsson, A. M. Haimovich, and M. Coulon: "Direct Localization for Massive MIMO," *IEEE Trans. on Signal Process.*, Vol. 65, No. 10, pp. 2475–2487, May 2017.
- [28] Z. Fu, K. Ren, J. Shu, X. Sun, and F. Huang: "Enabling Personalized Search over Encrypted Outsourced Data with Efficiency Improvement," *IEEE Trans. on Parallel and Distrib. Systems*, Vol. 27, No. 9, pp. 2546–2559, Sept. 2016.
- [29] T. S. Rappaport, *Wireless Communications: Principles and Practice*, Prentice Hall- PTR, 2001.
- [30] A. Goldsmith, *Wireless Communications*, U.K., Cambridge Univ. Press, 2004.
- [31] A. Bazzi, D. T. M. Slock, and L. Meilhac: "Efficient Maximum Likelihood Joint Estimation of Angles and Times of Arrival of Multiple Paths," *IEEE Globecom Workshops*, San Diego, pp. 1–7, Dec. 2015.
- [32] T. J. Shan, M. Wax, and T. Kailath: "On spatial smoothing for direction-of-arrival estimation of coherent signals," *IEEE Trans. on Acoustics, Speech, and Signal Process.*, Vol. 33, No. 4, pp. 806–811, Aug. 1985.
- [33] H. Krim and M. Viberg: "Two decades of array signal processing research: the parametric approach," *IEEE Signal Process. Mag.*, Vol. 13, No. 4, pp. 67–94, July 1996.

- [34] H. L. Van Trees, *Detection Estimation and Modulation Theory - Part IV: Optimum Array Processing*, John Wiley & Sons, Inc., New York, U.S.A., 2002.
- [35] L. Bernadó, T. Zemen, F. Tufvesson, A. F. Molisch, and C. F. Mecklenbräuker: "Delay and Doppler Spreads of Nonstationary Vehicular Channels for Safety-Relevant Scenarios," *IEEE Trans. Veh. Technol.*, Vol. 63, No. 1, pp. 82–93, Jan. 2014.
- [36] R. H. Clarke: "A statistical theory of mobile-radio reception," *The Bell System Technical Journal*, Vol. 47, No. 6, pp. 957–1000, July-Aug. 1968.